1. Additional Experimental Results

Figure S1 shows the accommodative response to the random step sequence for subject #3. The accommodation and relaxation tendencies were similar to those of subjects #1 and #2 but the comfortable accommodative range (amplitude) in the TL was smaller for subject #3 compared to other subjects due to the higher age. As can be seen, accommodation follows the induced defocus correctly from 1° to 6° eccentricity but with a reduced amplitude with increasing eccentricity. When at 7° and beyond, accommodation could no longer follow in the correct direction.
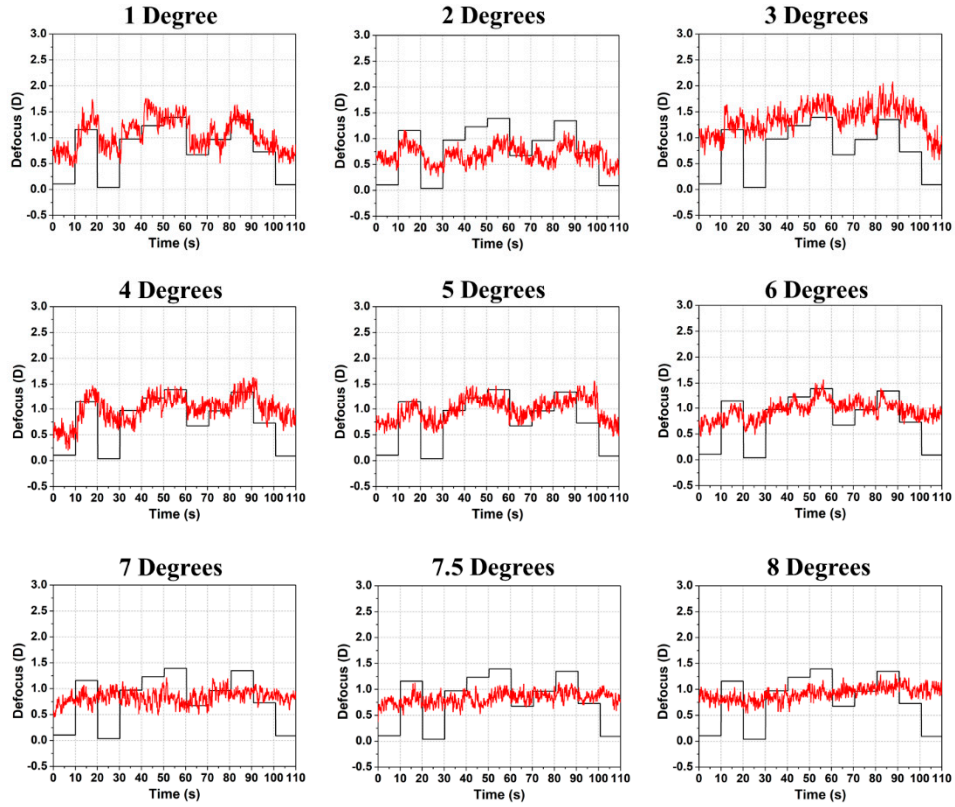

Figure S1. Induced defocus sequence by the TL (black line) and accommodation response (red line) as a function of time for subject #3 for increasing radial eccentricity from 1° to 8°. The induced defocus is shown with opposite sign to ease comparison.

Figure S2 shows how other Zernike terms changes along defocus during the step changes in the TL for subject #1. As can be seen defocus is the more dominant one while very minor change in astigmatism (Z_3 and Z_5) and spherical aberration Z_{12} has been noticed. More details about Figure S2 have been given in the main manuscript. In Figure S2 same step changes were made in the TL as Figure 2(a) for subject #1.
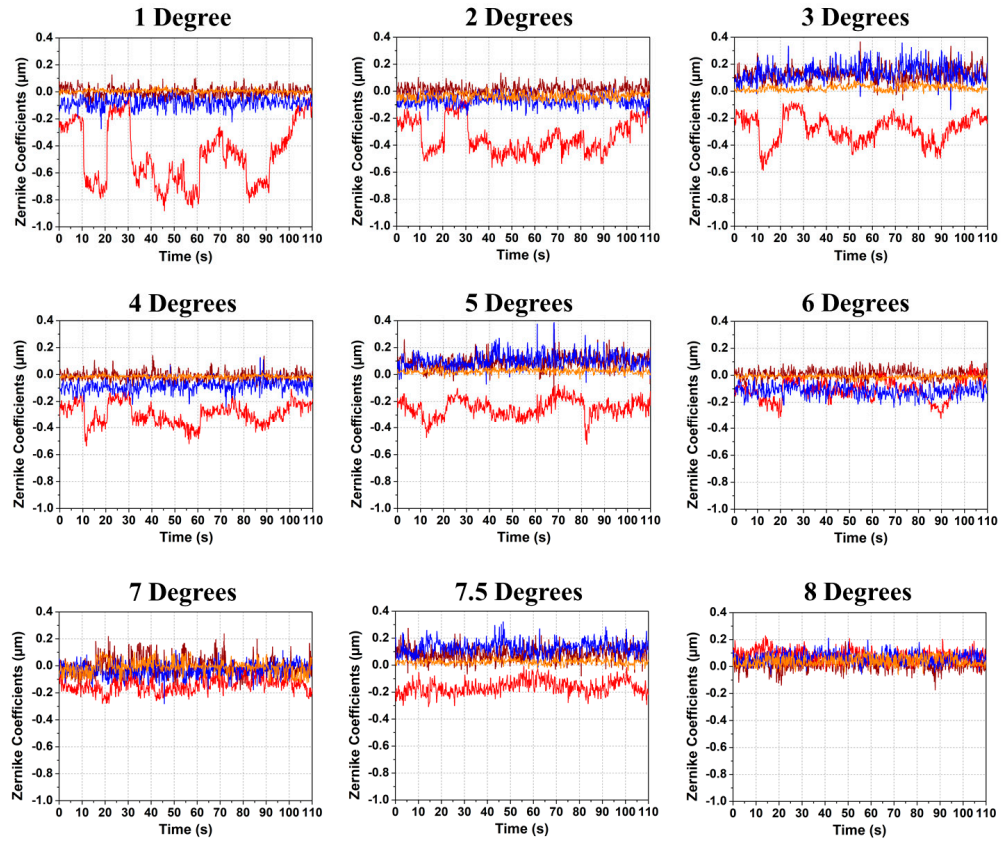
Figure S2. Individual Zernike coefficients in response to induced TL defocus changes for subject #1 for defocus Z_4 (red line), astigmatism Z_3 and Z_5 (brown and blue lines), and spherical aberration Z_{12} (orange line).

Figure S3 shows the accommodative response with the random defocus step changes for myopic subject #5. Like the other subjects from different groups of emmetropes, mild myopes and myopes, subject #5 was also able to accommodate in the correct direction up to 6°. As subject #5 was comparatively young (23), the comfortable accommodative range in the TL was larger for this subject compared to others and the accommodative response is clearly noticeable and compensated at lower eccentricity (1°, 2°) while with increased eccentricity the accommodative amplitude reduced as expected. At 7° and beyond there was no accommodative response in the correct direction anymore though the eye tried to act with the induced defocus.
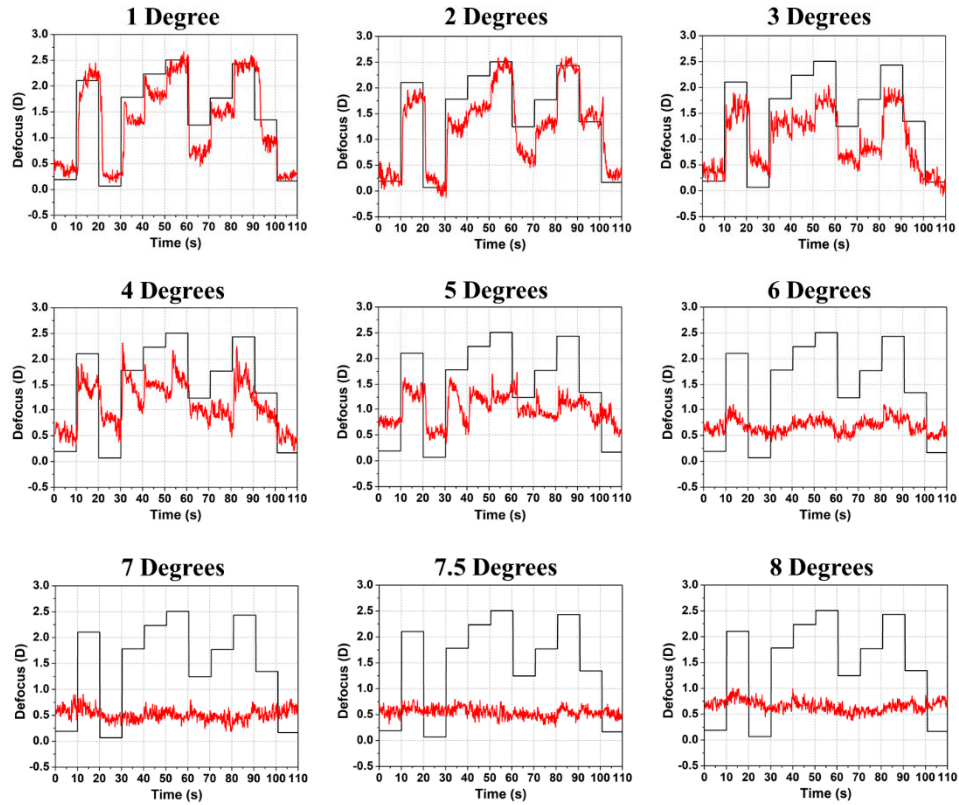
Figure S3. Induced defocus sequence by the TL (black line) and accommodation response (red line) as a function of time for subject #5 for increasing radial eccentricity from 1° to 8°. The induced defocus is shown with opposite sign to ease comparison.

2. Tunable Lens Aberrations

Any vertical-mounted liquid lens is prone to coma due to gravity so there is a risk that the TL may introduce undesired aberrations in the system. It has been inspected visually and by means of wavefront measurements with the HS-WFS but no conceivable reduction in image quality or wavefront beyond the desired defocus was found. The possible change of higher-order aberrations was also examined by the TL itself when changing power using the setup shown in Figure S4. In all cases these changes were negligible, and the defocus changes were found to be highly dominating.
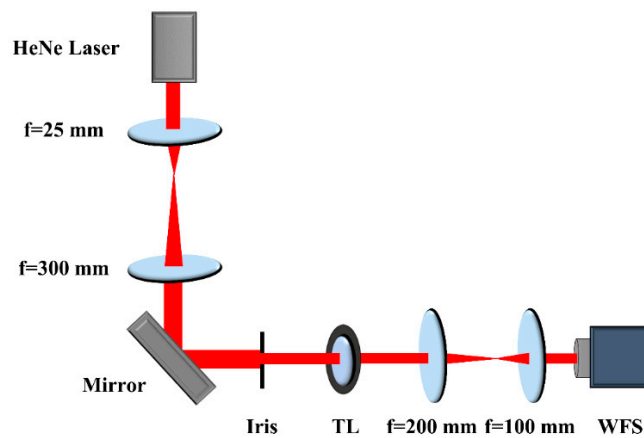

Figure S4. Schematic of setup to test Zernike coefficient changes in response to defocus changes of the TL monitored in a plane that is conjugate to the HS-WFS. An expanded collimated HeNe (633 nm) laser beam was used for the illumination. The iris was set to a beam diameter of 4.5 mm corresponding to the largest eye pupil used in this study.

The outcome of this verification test is shown in Figure S5 using the same random sequence of defocus changes of the TL as used during visual experiments of subject #1. Resulting changes of selected Zernike coefficients are shown in Figure S5(a) and, excluding the defocus term, a magnified view of coefficients in Figure S5(b). As can be seen, the defocus coefficient C_2^0 that scales the polynomial $Z_4 = Z_2^0$ is highly dominant. The enlarged view in Figure S5(b), note the different vertical scale, shows that small changes in other Zernike terms are present, resulting from a physical change, or from the truncation of the Zernike series to 4th order. As expected, there are very small changes of coma and astigmatism but essentially no change of spherical aberration. The largest change of coma and astigmatism happens when the defocus step is large (at 10 s, 20 s, 150 s and 190 s). The change of the coma and astigmatism coefficients is less than 0.2% of the Zernike defocus change.
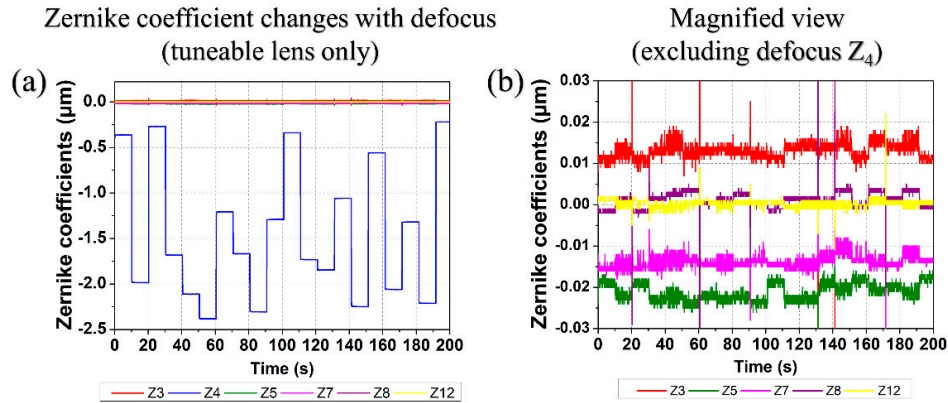

Figure S5. Changes of Zernike coefficients as a result of a random sequence of defocus changes generated with the TL as measured with the HS-WFS including up to 4th radial Zernike order. In (a) astigmatism (Z_3, Z_5), defocus (Z_4), spherical (Z_{12}), and coma (Z_7, Z_8) are all included on a common scale. In (b) defocus has been removed, and the vertical scale adjusted to reveal minute changes in the remaining Zernike coefficients when defocus changes.

3. Blink Removal

Removal of blinks can be challenging. A Matlab™ code was developed to remove blink-induced spikes from the HS-WFS measurements without deteriorating the relevant data. One example is given below.
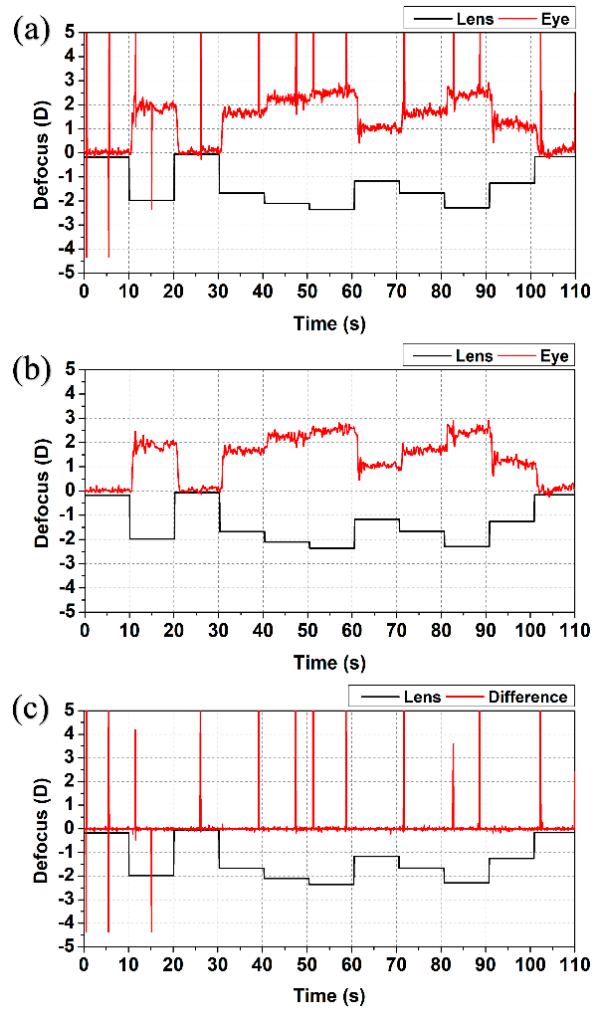
Figure S6. Analysis of blink removal with a Matlab™ code using (a) raw defocus data from the HS-WFS to obtain the (b) blink-filtered results. In (c) the difference between raw data and blink-corrected data shows no significant impact outside of the blink-induced spikes. Note that the sign of TL response has not been swapped here as it is in the main manuscript.

Figure S6 shows defocus data (from the HS-WFS defocus coefficient) before blink removal in Figure S6(a) and after blink removal in Figure S6(b). The example also includes a difference plot in Figure S6(c) to visualize the impact on the data before and after blink removal. It effectively isolates the blink-related peaks in the defocus data without impacting results elsewhere.